

**SYNTHESIS, CHARACTERISATION AND  
DETERMINATION OF MESOPHASE  
TRANSITION OF CYCLOTRIPHOSPHAZENE  
DERIVATIVES WITH AZO LINKING UNIT**

**MIYEKO LOTUS LOH LEH CHIING**

**UNIVERSITI SAINS MALAYSIA**

**2017**

**SYNTHESIS, CHARACTERISATION AND  
DETERMINATION OF MESOPHASE  
TRANSITION OF CYCLOTRIPHOSPHAZENE  
DERIVATIVES WITH AZO LINKING UNIT**

by

**MIYEKO LOTUS LOH LEH CHIING**

**Thesis submitted in fulfilment of the  
requirements for the Degree of  
Master of Science.**

**July 2017**

## **ACKNOWLEDGEMENT**

My greatest appreciation and gratitude goes to my supervisor, Associate Professor Dr. Melati Khairuddean, for her guidance and supervision since the beginning of this research. Above all, thank you for the time and commitment you have provided to me and your fellow students.

I would also like to thank the University for the facilities and space provided to complete this research. In addition to that, I am most grateful and humbled for the financial assistance that the university has graciously provided. Also to all the staffs for their diligence that helped propel this research forward, I thank you.

To my family and loved ones who provided me with so much physical and emotional support, I thank you for standing by me throughout this journey.

And finally to my dear friends and respected colleagues, what a ride! Thank you for the wonderful memories and bond we shared.

## TABLE OF CONTENTS

Acknowledgement	ii
Table of Contents	iii
List of Figures	vii
List of Tables	x
List of Schemes	xii
List of Abbreviations	xiii
Abstrak	xv
Abstract	xvi

### CHAPTER 1 INTRODUCTION

1.1	Research Background - Liquid Crystal	1
1.1.1	Classification of LCs	1
1.1.2	Basic concepts of LCs	4
1.1.3	Mesomorphic Azobenzene Molecules	
1.1.3(a)	Monoazo linking unit	5
1.1.3(b)	Bisazo linking unit	8
1.1.3(c)	Multiple different linking units	9
1.2	Cyclotriphosphazene	12
1.3	Problem Statement	16
1.4	Objectives	17
1.5	Scope of Study	17

### CHAPTER 2 METHODOLOGY

2.1	Chemicals	18
-----	-----------	----

2.2	Instruments	
2.2.1	Elemental Analysis	18
2.2.2	Infrared (IR) Spectroscopy	18
2.2.3	Nuclear Magnetic Resonance (NMR) Spectroscopy	19
2.2.4	Melting Point	19
2.2.5	Polarised Optical Microscopy (POM)	19
2.2.6	Differential Scanning Calorimetry (DSC)	19
2.3	Synthesis Method	20
2.3.1	Synthesis of 4,4'-(diazene-1,2-diyl)diphenol, <b>1</b>	22
2.3.2	General procedure for the alkylation of compounds <b>2a-f</b>	23
2.3.3	Synthesis of 4-(4-Nitrophenylazo) phenol, <b>3</b>	26
2.3.4	General procedure for the alkylation of compounds <b>4a-c</b>	27
2.3.5	General procedure for the reduction of compounds <b>5a-c</b>	29
2.3.6	General procedure for the synthesis of compounds <b>6a-c</b>	31
2.3.7	General procedure for the synthesis of monosubstituted cyclotriphosphazenes <b>7a-c</b>	33
2.3.8	General procedure for the synthesis of hexasubstituted cyclotriphosphazenes <b>7d-f</b>	35
2.3.9	General procedure for the synthesis of monosubstituted cyclotriphosphazenes <b>8a-c</b>	37

2.3.10	General procedure for the synthesis of hexasubstituted cyclotriphosphazenes <b>8d-f</b>	38
--------	--	----

### **CHAPTER 3 RESULTS AND DISCUSSION**

3.1	Spectral Discussion	39
3.1.1	Monoazobenzene intermediates	40
3.1.2	Bisazobenzene intermediates	49
3.1.3	Mono- and hexa-substituted cyclotriphosphazenes	58
3.2	Syntheses and Mechanism	
3.2.1	Monoazobenzene intermediates	71
3.2.2	Bisazobenzene intermediates	73
3.2.3	Mono- and hexa-substituted cyclotriphosphazenes	75
3.3	Determination of Mesophase Properties <i>via</i> POM and DSC	77
3.3.1	Mesophase properties of monoazobenzene intermediates	77
3.3.2	Mesophase properties of bisazobenzene intermediates	84
3.3.3	Mesophase properties of mono- and hexa-substituted cyclotriphosphazenes	90
3.4	Structure-Mesogenic Property Relationship	92
3.4.1	Influence of terminal groups	92
3.4.2	Influence of alkoxy chain length	93
3.4.3	Influence of linking group	93

### **CHAPTER 4 CONCLUSION**

4.1	Recommendation for Future Work	96
-----	--------------------------------	----

**REFERENCES**

97

**APPENDICES**

## LIST OF FIGURES

		Page
Figure 1.1	Comparison of the arrangement of molecules in crystal, liquid crystal and liquid phases	1
Figure 1.2	Classification of liquid crystals	2
Figure 1.3	Alignment of molecules in different liquid crystal phases	3
Figure 1.4	Molecular structure of a typical liquid crystal molecule	4
Figure 1.5	The structure of substituted cyclotriphosphazene	13
Figure 3.1	Overlay IR spectra of monosubstituted <b>2a</b> and disubstituted <b>2d</b>	41
Figure 3.2	Level of activation in electron donor substituents	43
Figure 3.3	DEPT spectra of compound <b>2a</b>	45
Figure 3.4	COSY spectrum of compound <b>2a</b>	47
Figure 3.5	HSQC spectrum of compound <b>2a</b>	48
Figure 3.6	Overlay IR spectra of <b>4a</b> and <b>5a</b>	50
Figure 3.7	Overlay IR spectra of <b>6a-6c</b>	53
Figure 3.8	DEPT spectra of compound <b>6c</b>	54
Figure 3.9	COSY spectrum of compound <b>6c</b>	57
Figure 3.10	HSQC spectrum of compound <b>6c</b>	58
Figure 3.11	Overlay IR spectrum of <b>7b</b> and <b>7d</b>	59
Figure 3.12	DEPT spectra of compound <b>7c</b>	61
Figure 3.13	DEPT spectra of compound <b>7e</b>	62
Figure 3.14	HSQC spectrum of compound <b>7c</b>	63



Figure 3.15	HSQC spectrum of compound <b>7c</b>	64
Figure 3.16	COSY spectrum of compound <b>7e</b>	65
Figure 3.17	HSQC spectrum of compound <b>7e</b>	66
Figure 3.18	<sup>31</sup> P NMR of all phosphorus containing compounds	69
Figure 3.19	Mechanism during (i) diazotisation; (ii) formation of phenolate ion; (iii) azo coupling reaction.	72
Figure 3.20	Mechanism for alkylation	73
Figure 3.21	Mechanism for reduction	75
Figure 3.22	Mechanism for mono-substitution reaction of cyclotriphosphazene	76
Figure 3.23	POM photograph of compound <b>2d</b> showing: (a) Nematic droplets during heating at 101.3°C and (b) Nematic four-point-brushes during cooling at 101.1°C. (Magnification of 20 · 0.50)	79
Figure 3.24	POM photograph of compound <b>2e</b> showing: (a) focal conic fan formation of SmA during heating at 108.8°C and (b) SmA battonets during cooling at 100.9°C (Magnification of 20 · 0.50)	80
Figure 3.25	POM photograph of compound <b>2f</b> showing: (a) SmC circular bubbles texture turning into marbled schlieren texture during heating at 110°C and (b) SmC circular bubbles texture during cooling at 107.7°C. (Magnification of 20 · 0.50)	80
Figure 3.26	DSC thermogram of compound <b>2d</b>	82
Figure 3.27	DSC thermogram of compound <b>2e</b>	83

Figure 3.28	DSC thermogram of compound <b>2f</b>	83
Figure 3.29	POM photograph of compound <b>4a</b> showing: (a) Nematic schlieren texture during cooling at 88.5°C; (b) Sm B rod-like grains during cooling at 80.7°C and (c) Sm B lancelets along with the rod-like grains at 79.2°C. (Magnification of 20 · 0.50)	86
Figure 3.30	POM photograph of compound <b>4b</b> showing: (a) SmA focal conic domains during heating at 91.6°C and (b) SmA focal conic fan formation during cooling at 85.1°C. (Magnification of 20 · 0.50)	87
Figure 3.31	POM photograph of compound <b>4c</b> showing: (a) SmA focal conic domains during heating at 82.5°C and (b) SmA focal conic fan formation during cooling at 73.8°C. (Magnification of 20 · 0.50)	87
Figure 3.32	DSC thermogram of compound <b>4a</b>	89
Figure 3.33	DSC thermogram of compound <b>4b</b>	89
Figure 3.34	DSC thermogram of compound <b>4c</b>	90

## LIST OF TABLES

		<b>Page</b>
Table 3.1	Summary of $^1\text{H}$ NMR chemical shifts in the aromatic region for <b>2a-f</b>	42
Table 3.2	Summary of $^{13}\text{C}$ NMR chemical shifts at the aromatic region for <b>2a-f</b>	42
Table 3.3	Comparison of $^1\text{H}$ -NMR, COSY ( $^1\text{H}$ - $^1\text{H}$ ) and HSQC ( $^1\text{H}$ - $^{13}\text{C}$ ) data for <b>2a</b>	46
Table 3.4	Summary of $^1\text{H}$ NMR chemical shifts for <b>4a-c</b> and <b>5a-c</b>	52
Table 3.5	Summary of $^{13}\text{C}$ NMR chemical shifts for <b>4a-c</b> and <b>5a-c</b>	52
Table 3.6	Summary of $^1\text{H}$ NMR chemical shifts at the aromatic region for <b>6a-c</b>	55
Table 3.7	Summary of $^{13}\text{C}$ NMR chemical shifts at the aromatic region for <b>6a-c</b>	55
Table 3.8	Comparison of $^1\text{H}$ -NMR, COSY ( $^1\text{H}$ - $^1\text{H}$ ) and HSQC ( $^1\text{H}$ - $^{13}\text{C}$ ) data for <b>6c</b>	56
Table 3.9	Summary of $^1\text{H}$ NMR chemical shifts at the aromatic region for <b>7a-f</b>	60
Table 3.10	Summary of $^{13}\text{C}$ NMR chemical shifts at the aromatic region for <b>7a-f</b>	60
Table 3.11	Comparison of $^1\text{H}$ -NMR, COSY ( $^1\text{H}$ - $^1\text{H}$ ) and HSQC ( $^1\text{H}$ - $^{13}\text{C}$ ) data for <b>7c</b>	67
Table 3.12	Comparison of $^1\text{H}$ -NMR, COSY ( $^1\text{H}$ - $^1\text{H}$ ) and HSQC	68

(<sup>1</sup>H-<sup>13</sup>C) data for **7e**

Table 3.13	Elemental analyses results of selected compounds	70
Table 3.14	Phase sequence for monoazobenzene intermediates	78
Table 3.15	DSC data of mesogenic monoazobenzene compounds upon heating	81
Table 3.16	DSC data of mesogenic monoazobenzene compounds upon cooling	81
Table 3.17	Phase sequence for bisazobenzene intermediates	85
Table 3.18	DSC data of mesogenic bisazobenzene compounds upon heating	88
Table 3.19	DSC data of mesogenic bisazobenzene compounds upon cooling	88
Table 3.20	Phase sequence for final compounds <b>7a-f</b>	91

## LIST OF SCHEMES

		Page
Scheme 1	Synthesis pathway for azo coupling of monoazobene, <b>2a-f</b>	20
Scheme 2	Synthesis pathway for azo coupling of bisazobenzene, <b>6a-c</b>	20
Scheme 3	Synthesis pathway of cyclotriphosphazene products with monoazo linking unit for mono-substituted, <b>7a-c</b> and hexa-substituted, <b>7d-f</b>	21
Scheme 4	Synthesis pathway of cyclotriphosphazene products with two azo linking unit for mono-substituted, <b>8a-c</b> and hexa-substituted, <b>8d-f</b>	21

## LIST OF ABBREVIATIONS

CDCl <sub>3</sub>	Deuterated chloroform
DMSO-d <sub>6</sub>	Deuterated dimethyl sulfoxide
DCM	Dichloromethane
H <sub>2</sub> O	Distilled water
EtOH	Ethanol
EtOAc	Ethyl acetate
MeOH	Methanol
THF	Tetrahydrofuran
CTP	Hexachlorocyclotriphosphazene
HCl	Hydrochloric acid
Ph-OH	Phenol
KOH	Potassium hydroxide
K <sub>2</sub> CO <sub>3</sub>	Potassium carbonate
CH <sub>3</sub> COONa	Sodium acetate
NaOH	Sodium hydroxide
NaNO <sub>2</sub>	Sodium nitrite
Na <sub>2</sub> S.9H <sub>2</sub> O	Sodium sulfide nonohydrate
Et <sub>3</sub> N	Triethylamine
FT-IR	Fourier Transform Infrared Spectroscopy
<sup>1</sup> H NMR	Proton Nuclear Magnetic Resonance
<sup>13</sup> C NMR	Carbon Nuclear Magnetic Resonance

COSY	Correlated spectroscopy
HSQC	Heteronuclear Single Quantum Coherence
TLC	Thin Layer Chromatography
POM	Polarised Optical Microscope
DSC	Differential Scanning Calorimetry
MHz	mega hertz
Hz	hertz
J	coupling constant
s	singlet
d	doublet
t	triplet
m	multiplet
ppm	parts per million
1D	one dimensional
2D	two dimensional
Cr	crystal
SmA	Smectic A
SmB	Smectic B
SmC	Smectic C
N	nematic
I	isotropic

**SINTESIS, PENCIRIAN DAN PENENTUAN PERUBAHAN  
MESOFASA BAGI TERBITAN SIKLOTRIFOSFOZENA DENGAN  
UNIT PENYAMBUNG AZO**

**ABSTRAK**

Siri bahan perantara telah disintesis melalui tindak balas pengkupelan azo bagi menghasilkan sebatian alkil dengan satu unit penyambung azo, **2a-c** dan dengan dua unit penyambung azo, **5a-c**. Bahan perantara ini seterusnya mengalami tindak balas penukargantian mono dan penukargantian heksa dengan siklotrifosfazena bagi menghasilkan siri sebatian akhir **7a-f**. Kesemua sebatian ini telah dicirikan secara FT-IR (infra merah), spektroskopi 1D dan 2D NMR (Resonan Magnetik Nuklear), dan analisa unsur CHN. Bahan perantara **2d-f** dan **4a-c** didapati adalah mesogenik dengan fasa nematik dan smektik melalui mikroskop terkutub optik (POM). Endoterma daripada kalorimeter pengimbasan perbezaan (DSC) menunjukkan peralihan fasa kristal-mesofasa, mesofasa-mesofasa kalau ada, dan mesofasa-isotropik ketika kitaran pemanasan; dan sebaliknya ketika kitaran penyejukan. Sifat mesofasa dihubung kait dengan pengaruh kumpulan terminal, kepanjangan rantaian alkoksi dan unit penyambung. Sifat smektogenik didapati lebih ternyata dengan rantaian alkoksi yang semakin panjang. Sebatian tertukarganti mono- dan heksa-, **7a-f** adalah bukan mesogenik. Hal ini adalah kerana pengenalan siri bahan perantara yang tidak mesogenik kepada siklotrifosfazena.



**SYNTHESIS, CHARACTERISATION AND DETERMINATION OF  
MESOPHASE TRANSITION OF CYCLOTRIPHOSPHAZENE  
DERIVATIVES WITH AZO LINKING UNIT**

**ABSTRACT**

A series of intermediates were synthesised *via* azo coupling reactions to give the alkylated compounds with one azo linking unit, **2a-c** and with two azo linking units, **5a-c**. These intermediates were subjected to further monosubstitution and hexasubstitution reactions with cyclotriphosphazene to produce a series of final compounds **7a-f**. These compounds were characterised using FT-IR (Fourier Transform Infrared), 1D and 2D NMR (Nuclear Magnetic Resonance) spectroscopy and CHN elemental analysis. Intermediates **2d-f** and **4a-c** were found to be mesogenic with nematic and smectic phases, as determined under the POM (Polarised Optical Microscopy). The endotherms obtained from the DSC (Differential Scanning Calorimetry) showed the respective phase transitions of crystal-mesophase, mesophase-mesophase if any, and mesophase-isotropic phases during the heating cycle; and *vice versa* during the cooling cycle. The influence of terminal groups and linking groups on mesogenic properties was discussed. Smectogenicity was found to be enhanced with increasing alkoxy chain length. Mono- and hexa-substituted compounds **7a-f** were found to be non-mesogenic. It was concluded that the introduction of non-mesogenic side arms resulted in the lack of liquid crystalline properties in **7a-f**.

## CHAPTER 1

### INTRODUCTION

#### 1.1 Research background – Liquid Crystal

Since the first discovery of liquid crystal (LC) molecules by Reinitzer in 1888, extensive research has been done to investigate the physical and chemical properties of LCs (Reinitzer, 1989), leading to the creation of new materials with the fascinating application. Liquid crystal is an intermediate phase between liquid and solid (Chandrasekhar, 1992); a state of matter that has both the properties of isotropic liquid and solid crystal (Demus et al., 1998). Liquid crystal intermediate state(s) are called mesophase(s), which has orientational order but no positional order, as illustrated in Figure 1.1.

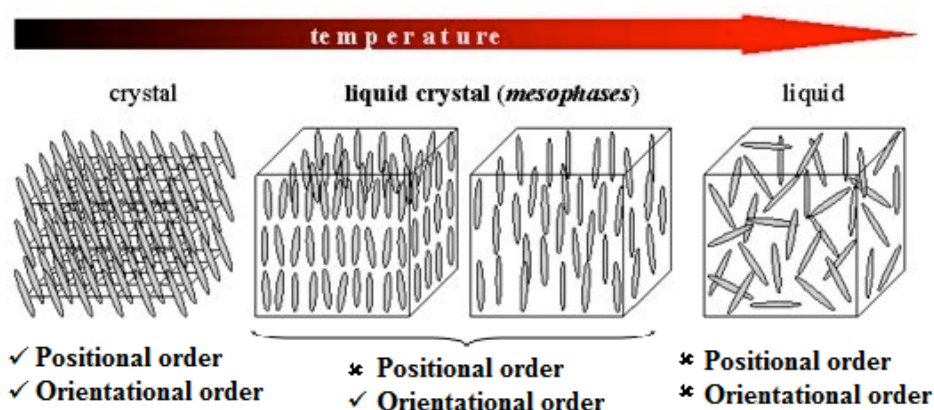


Figure 1.1: Comparison of the arrangement of molecules in the crystal, liquid crystal and liquid phases (Shruti, 2003).

##### 1.1.1 Classification of LCs

There are two distinct types of liquid crystal for the organic compounds, which are thermotropic and lyotropic. Thermotropic LC is temperature dependent in which the LC mesophase(s) appear by heating above the solid phase or cooling from the liquid phase (Kašpar *et al.*, 2004). The heating temperature from solid to liquid

crystal phase is called the *melting point* while the temperature from liquid crystal to isotropic phase is called the *clearing point*. Molecules with liquid crystal phase(s) which appear in both the heating and cooling cycles are regarded as *enantiotropic*, while the mesophases that appear only during cooling or heating cycle are known as *monotropic*. The thermotropic molecules are classified into three main shapes which are calamitic (rod-like), discotic (disk-like) and banana-shaped which usually give rise to mesophase(s). On the other hand, the lyotropic liquid crystal is concentration and temperature dependent, whereby the liquid crystal mesophase is formed only when the molecule is mixed with a solvent (Fisch and Kumar, 2001). For such compounds, the concentration of the solution is just as important as the temperature in determining whether a liquid crystal phase is stable. The classes of LCs are outlined in Figure 1.2. Determination of liquid crystal mesophase(s) using a polarised optical microscope (POM) show different textures depending on the molecules. Calamitic liquid crystal usually exhibits the nematic and smectic phases, while the discotic tend to form columnar and nematic phases (Collings and Hird, 1998).

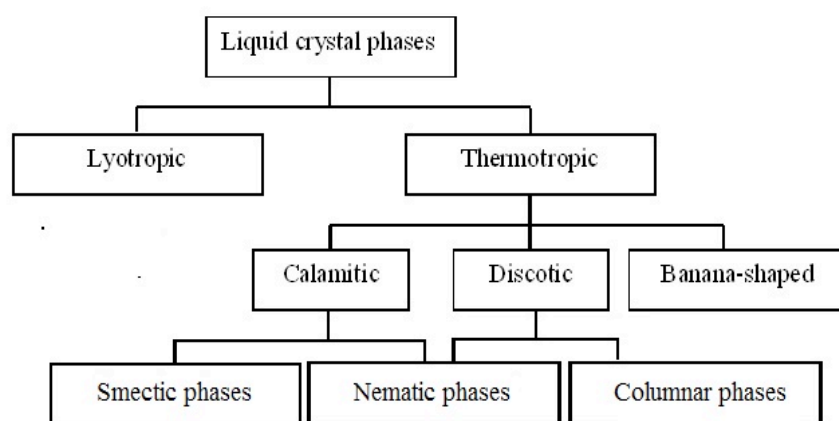


Figure 1.2: Classification of liquid crystals (Gray, 1983)

The nematic phase is characterised by molecules that have no positional order but tend to point in the same direction while the smectic phase is found at lower temperatures than the nematic, having the orientational order, but also tend to align themselves in layers or planes that can slide over one another. The most known are the smectic A and C phases. The smectic A phase is a linear phase, in which the molecules are perpendicular to the layers whereas smectic C phase is a tilted phase (Gray, 1984). The schematic arrangement of molecules is illustrated in Figure 1.3.

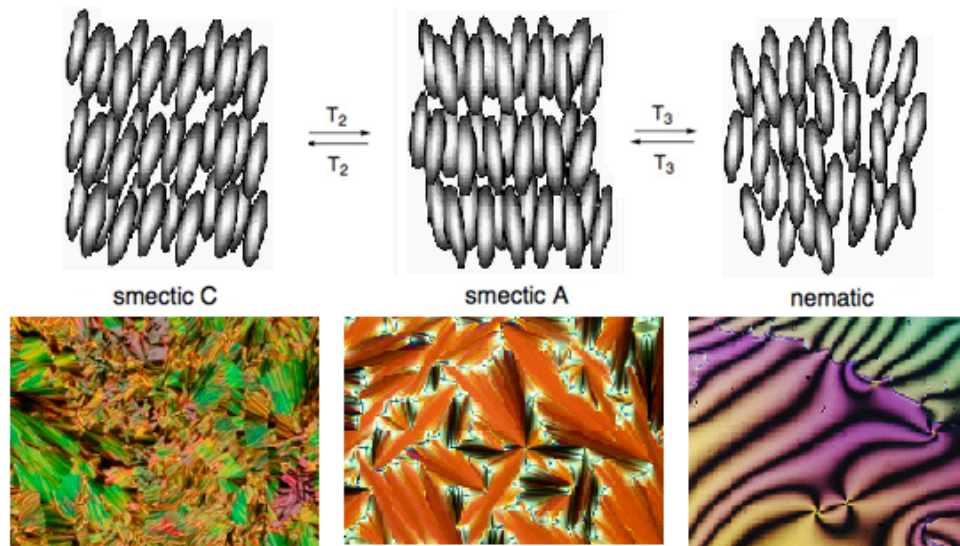


Figure 1.3: Alignment of molecules in different liquid crystal phases (Ocak *et al.*, 2009; Francescangeli and Samulski, 2010; Brown and Wolken, 1979).

Liquid crystal technology has shown a major effect in many areas of science and devices. Some applications of the thermotropic liquid crystal molecules include liquid crystal displays (LCD), electro-optical devices, thermometers, medical appliances, optical imaging and flame retardant substances (Kelly and O'Neill, 2000; Walter, 2003; Denis, 2006; Du *et al.*, 2006). On the other hand, lyotropic are significantly improving some technological aspects of cosmetics, soaps, food, crude oil and detergent production (Petrov, 1999).

### 1.1.2 Basic concepts of LCs

In 1922, Friedel described liquid crystal as rod- or disc-shaped molecules that favour a linear molecular arrangement (Brown, 1969). It is important that the molecule is fairly rigid, for at least some portion of its length, since it must maintain an elongated, thin and often flat shape (Kelker and Hatz, 1980). Branching (bilateral substitution) might disrupt the linearity of the molecule. It is important to choose the suitable core, linking unit or terminal group to obtain a mesogenic molecule. Molecular shape is important in self-assembly of a molecule which gives the impact on the ordering abilities of mesogenic molecules. It was reported that the ability to self-assemble depends on  $\pi$ - $\pi$  interactions and without distinct hydrophilic and hydrophobic regions, it is unlikely to self-assemble into liquid crystal phase (Foster, *et. al.*, 2006). The most common structure of a rod-like molecule consists of a core (usually one or two aromatic ring) which is attached to other core by linking units (Collings and Hird, 1997). Some of the molecules have a series of chain at the terminal end (Jeong *et al.*, 2007). Molecules that form liquid crystals have dipoles in their structure, often with a strong dipole towards the centre and a weak dipole towards the end of the molecules. Also, Vorländer suggested that only molecules broader than benzene were found to be mesomorphic (Sluckin *et al.*, 2004). The common molecular structure of the liquid crystal is as shown in Figure 1.4.

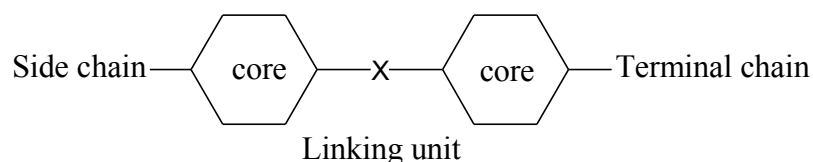


Figure 1.4: Molecular structure of a typical liquid crystal molecule (Khoo, 2007)

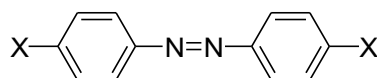
Linking units are normally structural units that connect one core to another, which maintain the linearity of the core while being compatible with the rest of the

structure. A linking unit between ring systems is to increase the length of the molecules and to alter the polarisability and flexibility of the molecules (Frenkel and Mulder, 1985). Compounds with linking groups are easier to synthesise compared to compounds with direct bonds because the linking group provides a point of link up in the synthesis. Some examples of the linkage groups are stilbene (-CH=CH-), ester (-COO-), Schiff base (-CH=N-), azo (-N=N-), acetylene (-C≡C-), and diacetylene (-C≡C-C≡C-). These groups can conjugate with phenyl rings, which enhance the polarisability, resulting in the increase of molecular length while maintaining the rigidity (Kelker and Hatz, 1980; Khoo, 2007) and restricting the freedom of rotation (Demus et. al., 1998).

### 1.1.3 Mesomorphic Azobenzene Molecules

#### (a) Monoazo linking unit

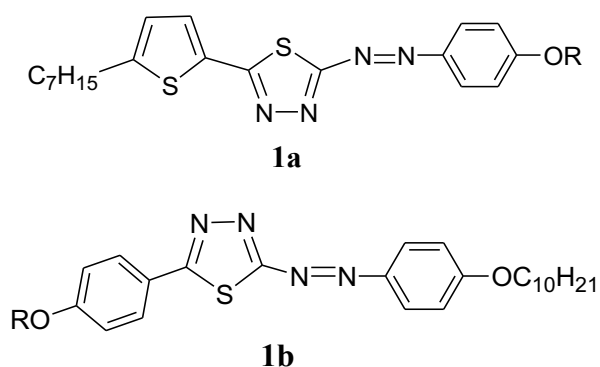
Azobenzene derivatives were among the first recognised groups of liquid crystalline molecules (Niezgoda and Galewski, 2013). As early as 1902, substituted mono azobenzenes with mesogenic properties have been synthesised (Kelker and Hatz, 1980).



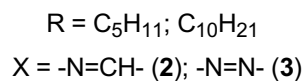
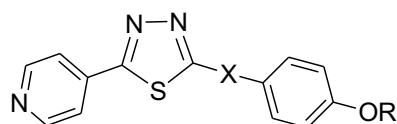
X = *n*-alkyl, chiral alkyl, OR, other substituents

Azo compounds usually give rise to stable mesophases. They are thermally very stable and appealing in the studies of photoinduced effects (Kašpar *et al.*, 2004; Prasad, 2001c). Previous investigations have reported on the mesomorphic azobenzenes effects of the molecular shapes, central linkage units, terminal substitutions and length of terminal chain on the mesomorphic properties.

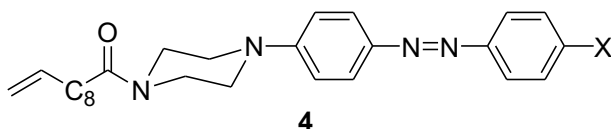
Parra *et al.* (1997) compared the Schiff base and azo linkages in the compounds and concluded that Schiff base linkage showed higher thermal stability than the latter due to the rigidity in the Schiff base linkage, which caused a higher rotational behaviour and more planar structure. Furthermore, stronger molecular interactions in Schiff base derivatives resulted in higher clearing temperatures compared to the azo derivatives. The effect of different ring units was also investigated, by synthesising the azo compounds, derived from phenyl- and thienyl-1,3,4-thiadiazole ring. The thiophene ring in series **1a** caused a molecular curvature that disturbed the formation of stable mesophases which resulted in series **1b** showing larger mesomorphic range than series **1a**.



The pyridine rings incorporated into a new series of azo compounds, **3**, were compared with their Schiff base analogues, **2**, as well as series **1** (Parra *et al.*, 1997). Series **3** showed nematic phase (monotropic) while **2** showed SmA (enantiotropic) phase. The differences in mesomorphic abilities between series **2** and **3** were attributed to the rigidity of the central linking unit. By comparing series **3** and **1**, it was concluded that compounds with the pyridine unit were not long enough or sufficiently polarisable to produce stable mesophases (Parra *et al.*, 2008).



Similarly, Nishiyama and Yamamoto (2015) highlighted the role of the central groups and the importance of rigidity in maintaining a stable mesophase. The azo and ester linking groups were compared and it was found that the azo group showed increased rigidity in the planar structure of the core, which resulted in a more stabilised mesophase. Lai and Lin (2000) synthesised the first series of piperazine-containing dye, **4**, with SmC phase and variation of mesogenic behaviour with different length of alkyl chains. SmC phase appeared with the introduction of a flexible chain length in compounds **4b-d**, as compared to SmA and nematic phases in compound **4a**. The increased chain length increases the range of SmC phase as well.

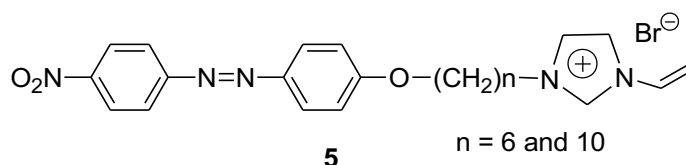


Lai *et al.* reported more smectogenic piperazine-containing dye and focused on the molecular arrangement study to analyse the interaction between the functional molecules, which influenced the stability and phase behaviour. It was found that the stabilisation of molecular stacking was affected by the polarity of the molecules (Lai *et al.*, 2001) and intermolecular hydrogen bonding (Lai *et al.*, 2002). Then, it was demonstrated that the H-bond interaction plays an important role in varied mesogenic behaviour (Lai *et al.*, 2004) for the azo dyes of different terminal alkyl chain length. They showed different mesogenic behaviour despite having the same rigid core. Stronger H-bond interaction in the shorter-chained molecule resulted in



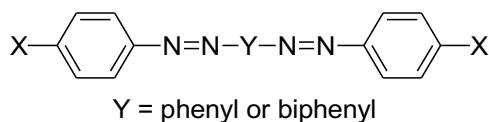
bending of the conformation of molecules while maintaining a layer, which led to the observation of SmA and nematic phase.

Zhang *et al.* (2011) reported the synthesis of new liquid crystals with the ionic liquid, **5** based on *p*-nitrobenzene with substituted vinylimidazolium ion group. It was found that the ionic interaction between imidazolium salts and the flexible chain stabilised the smectic A phase.



**(b) Bisazo linking unit**

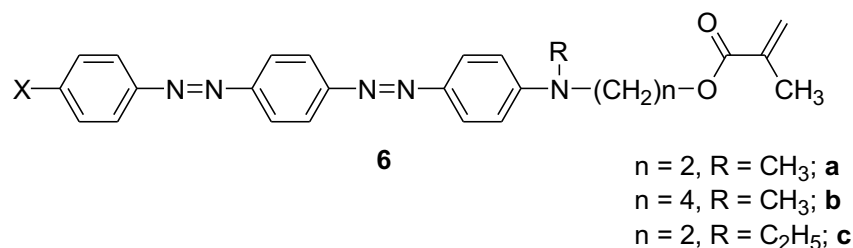
Synthesis of the mesomorphic phenyl-*p*-bisazobenzenes by Ritter and Halle (1928), biphenyl-*p*-bisazobenzenes by Bremer and Halle (1924) and Vorländer (1937), were among the first reported bisazobenzenes (Kelker and Hatz, 1980).



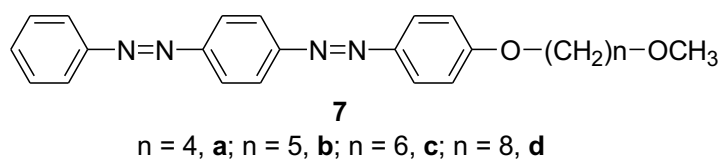
Bisazobenzenes have been prepared and investigated for optical storage applications (Cojocariu and Rochon, 2005; Meng *et al.*, 1997). Compared to its monoazobenzene analogues, bis-azobenzene chromophores are distinguished by a high anisotropy of molecular polarisability, which can lead to large photoinduced orders (Zheng *et al.*, 2007). The level of photoinduced birefringence per azo structure unit in bisazobenzene-based materials was reported to be five times larger and more stable than that in monoazobenzene (Meng *et al.*, 1997).

Cojocariu and Rochon (2005) investigated the effects of spacers and *N*-alkyl donor groups during the study of the mesogenic mono- and bis-azobenzenes. It was

found that by replacing a bulky group with a less bulky one, it increased the tendency towards smectic mesophase formation. The decreased in steric hindrance also resulted in a more compact packing of the molecules, which led to an increased in mesomorphic stability. Furthermore, increasing the length of spacers decreased the glass transition temperature.



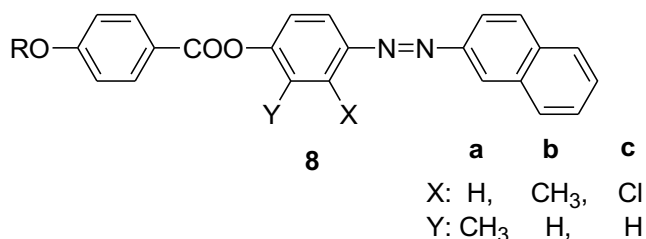
Salisu *et al.* (2011), Rahman *et al.* (2009) and Silong *et al.* (2009) have reported the synthesis of new calamitic liquid crystal material with bis-azobenzene moieties as a core. Compounds **7** exhibited enantiotropic mesogens, whereby the increased length of the terminal chain showed SmA and nematic mesophases. The core length of two azo groups with the increased in the terminal units and the presence of polar methoxy groups at the terminal end were believed to improve the enantiotropic behaviour, thermal stability and mesophase stability.



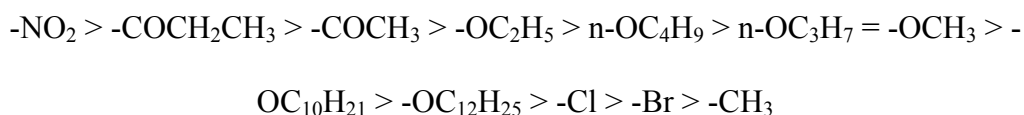
### (c) Multiple different linking units

Azo-containing compounds attached to other linking units such as ester, Schiff base and others were also reported. By introducing different linking groups, various mesophases arises. Prajapati has reported a series of mesogenic azo-esters containing naphthalene moiety and discussed the effects of lateral groups namely

methyl (Prajapati et al., 2000) and chloro (Prajapati *et al.*, 2003) group, at different positions. Series **8a** and **b** showed nematic phase. The lack of smectic phase can be explained by the increase in breadth due to the lateral methyl group on the central benzene ring and a coplanarity of the system due to steric interaction. The average thermal stabilities of **8b** were higher than those of series **8a** because the lateral methyl group was ortho to the –COO- central linkage. The –COO- was more flexible than –N=N- and this compensated for steric hindrance which resulted in a more compact packing of the molecules to stabilise the nematic phase. The lateral group efficiency order for the nematic phase stability are  $-H > -Cl > -CH_3$ .

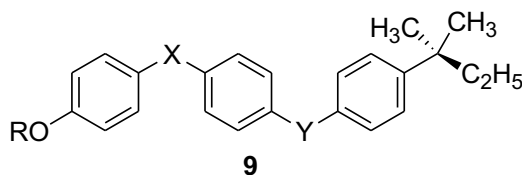


Dave and Menon (2000) have reported the synthesis of azo-ester dyes and evaluated the effect of different terminal substitutions. All compounds displayed nematic phase, whereby compounds with more polarisable terminal groups such as ketone end groups tend to exhibit smectic A phase compared to that of the *n*-alkoxy terminal moieties which exhibited smectic C phase. The group efficiency order for the nematic phase thermal stability is as shown below.



Similarly, more studies on the influence of the terminal substituents have been reported (Thaker and Kanojji, 2010; Thaker *et al.*, 2011), which compared the thermal stability of different central linkages in the synthesis of azo-esters and azo-

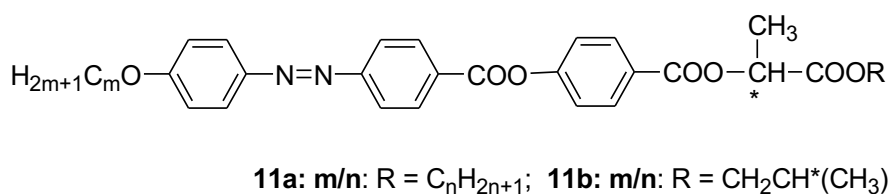
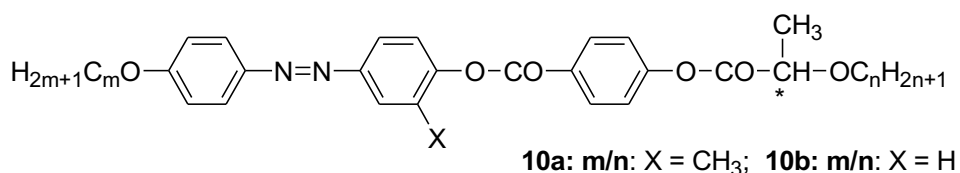
cinnamate with biphenyl moiety. The latter was found to be more thermally stable than the former. Another synthesis of mesogenic azo-ester and azomethine-ester series were also reported. It was found that the azomethine linkage caused an onset of smectic phase compared to the azo linkage (Patel and Dave, 2006).

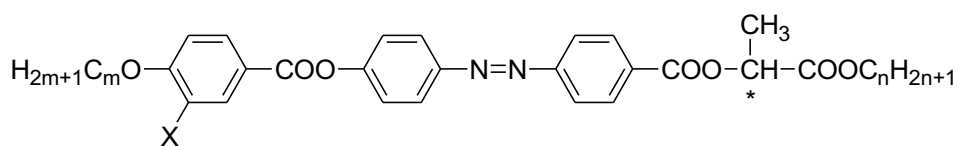


Series	X	Y
I	-COO-	-N=N-
II	-COO-	-CN=N-

where  $R = C_nH_{2n+1}$ ;  $n = 1-8, 10, 12, 14$  and  $16$

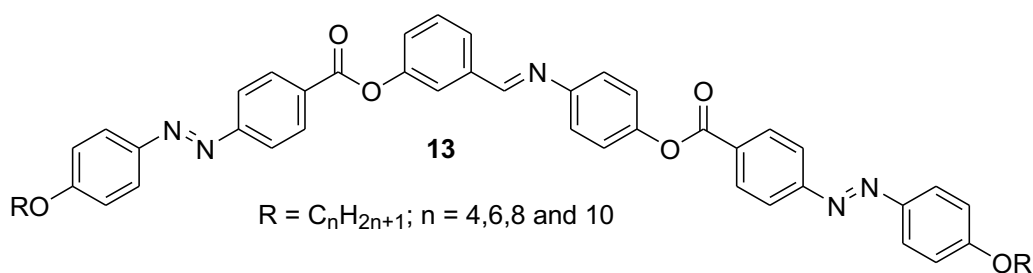
Kašpar *et. al* (2004) have reported six new series of azo-ester ferroelectric liquid crystalline compounds derived from chiral *S*-lactic acid as a terminal moiety. Effects of the azo group at different positions of the core unit and the methyl substitution were studied. The absence of smectic phases in series **10a m/n** and **12a m/n** was attributed to the lateral substitution which caused the steric hindrance and decreased the phase transition temperatures compared to the non-substituted series. There was a suppression of the ferroelectric phase when the azo group is placed closer to the chiral centre (series **12a m/n** and **12b m/n**).





**12a:** m/n: X = CH<sub>3</sub>; **12b:** m/n: X = H

Other than the conventional calamitic and discotic liquid crystal molecules, bent-core molecules are non-conventional liquid crystals known to exhibit liquid crystal behaviour even though their molecular geometry deviates from the classic disc or rod-shapes. The mesophases are labelled with the code letters B<sub>n</sub>, where n = 1-7, according to the sequence of their discovery, whereby ‘B’ represents bent, banana or boomerang. Prasad *et al.* (2001a) reported the first example of the azo-containing bent-core molecules. It was found that in compound **13**, the imine group was more conducive to mesomorphism compared to the azo and was more thermally stable. More novel bent-shaped azo compounds with liquid crystal properties were reported (Prasad, 2001b; Prasad and Jákli, 2004).



## 1.2 Cyclotriphosphazene

During the past decade, the area of organic, inorganic and organometallic chemistry has expanded rapidly, leading to the new area of material science. In line with these advances, the phosphorus-nitrogen chemistry has attracted a wide attention especially in the area of cyclotriphosphazenes which was extensively explored in the mid-1950's (Allcock, 1972). Hexachlorophosphazene is a hexa-

membered cyclic organophosphazene ring with the formula of  $(\text{NPCl}_2)_3$ . It is also known as cyclotriphosphazene, a ring compound consisting of alternating phosphorus and nitrogen atoms with two substituents attached to the phosphorus atoms, as shown in Figure 1.5.

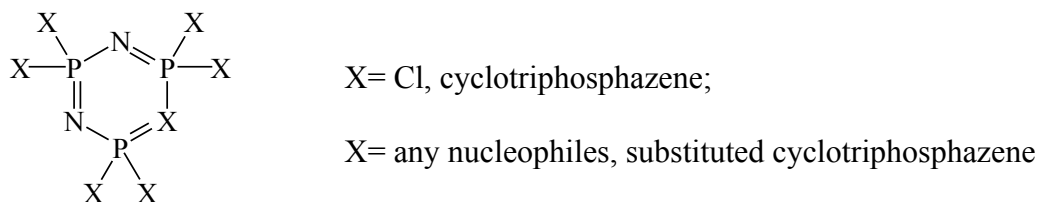


Figure 1.5: The structure of substituted cyclotriphosphazene

Much attention has been focused on these interesting compounds because they consist of inorganic backbones as well as organic side-chains. These compounds are chemically stable and synthetically versatile which enables the introduction of any side arm, R on phosphorus (Allcock and Kugel, 1965). Cyclotriphosphazene yields a broad range of materials with different physical and chemical properties by being readily attached to a variety of substituents (Singler, 1975; Allcock, 2004). Previous studies reported that substituents such as  $-\text{NH}_2$ ,  $-\text{OR}$ ,  $-\text{OC}_6\text{H}_5$  or fluorinated derivatives are able to enhance the oxidative and thermal stabilities (Lyon, 2002), exhibiting unusual thermal properties such as flame retardancy and self-extinguishability (Jaeger and Gleria, 1998). Cyclotriphosphazenes with different side arms have been studied extensively and due to their fascinating properties, they were used in commercial applications (Haiduc, 1970; Allcock, 1972b; Heal, 1980; Allen, 1987; Allen, 1990; Allcock, 2003).

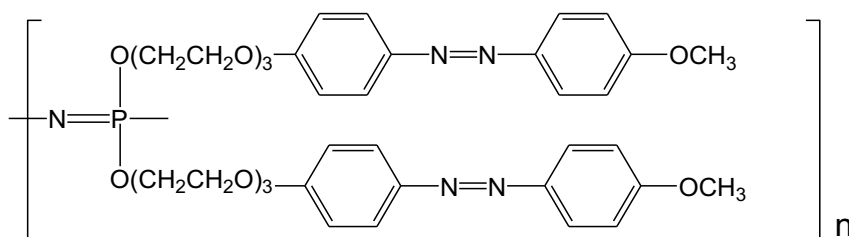
Halogen substances used to be the most effective substances as fire retardants until the National Institute of Standards and Technology (NIST) chemical search in 1990 deemed halides as too toxic and too hydrolytically unstable as fire

extinguishing agents (Pitts *et al.*, 1990). Although phosphorus and nitrogen-containing salts have long known to be effective fire suppressants, these salts are not regarded as clean fire extinguishant, making them not suitable for halogen replacement applications (Amrogowicz and Kordylewski, 1991).

In light of this, two active elements found in flame-retardants are phosphorus and nitrogen. The combination of these two elements in the same compound lead to a synergistic effect wherein the combined effect of two components is greater than a simple additive combination of their individual flame retardant effects. Consequently, this puts phosphazene materials in the limelight as high potential environmental friendly fire retardants (Allen, 1993). Other findings reported that the use of phosphazenes as halogen replacement agents are highly effective in flame suppression and have shown excellent potential in preventing explosion (Skaggs *et al.*, 1995).

Reports on liquid crystal phosphazenes have been published over the years, whereby their phase textures and transitions were studied and factors affecting mesomorphism were discussed. The general method of synthesising liquid crystal phosphazene includes the introduction of the mesogenic side chain(s) to a phosphazene backbone. Some of the early works reported the attachment of mesogenic molecules to a phosphazene ring *via a* flexible spacer group. Singler (1987) mentioned that Finkelmann and other workers were the first to demonstrate the coupling of a mesogenic group with a flexible spacer to a polymeric substrate in 1982. Kim and Allcock (1987) have successfully synthesised their first mesogenic polyphosphazene, **14** by linking the mesogenic aromatic azo unit to the polyphosphazene chain with tri(ethyleneoxide) spacer groups. From this, it was

concluded that LC behaviour was accessible by linking appropriate mesogenic groups to a polyphosphazene chain through a sufficiently flexible spacer unit.

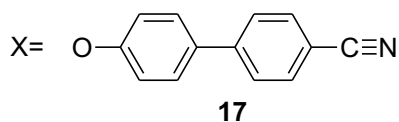
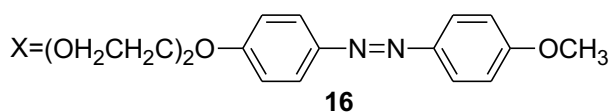
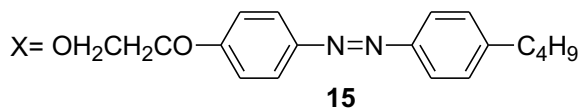
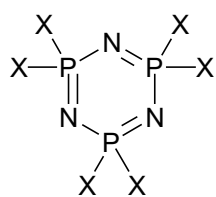


**14**

Reports on other mesogenic phosphazenes include compounds with cyclic trimer backbone, having different R groups attached to the side arms. Singler *et al.* (1987) observed the liquid crystal properties in mesogenic azo compounds attached to a cyclic trimer phosphazene backbone, with ethoxide spacer group, **15**. Allcock and Kim (1989) highlighted some liquid crystal inducing factors namely the role of terminal substituents, length and flexibility of the spacer unit and the influence of different phosphazene structures (cyclic trimer and polymeric phosphazenes). The molecules linked aromatic azo units with ethyleneoxy spacer groups to the cyclic trimer and high polymer, **16**.

However, Moriya *et al.* (1990) reported the introduction of mesogen to the phosphazene core without the flexible spacer unit. Although this work did not introduce an azobenzene unit to the phosphazene core, it is worth mentioning as they successfully reported the first case of mesogenic organocyclotriphosphazene, **17** without any spacer between the P-O linkage and the rigid core of mesogen.





Later, work on the mesogenic cyclic trimer molecules without spacer units continued to be published. The thermal stabilities with different side arms such as biphenyl groups (Moriya *et al.*, 1997) and Schiff bases (Moriya *et al.*, 1998) were compared and the order of stability (Moriya *et al.*, 2001) was concluded in the following order: phenylazobenzene > phenyliminomethylphenyl > biphenyl.

### 1.3 Problem Statement

Numerous cyclotriphosphazene liquid crystal molecules have been synthesised and characterised which has significantly enhanced the understanding of structure-property relationships and uncovered more molecules with unusual physical properties. In the search for improved properties, not many liquid crystal molecules with azo linking arms are widely explored, in particular, molecules of the azo linking unit attached to the cyclotriphosphazene core. The research is to investigate whether the series of substituted cyclotriphosphazene show any liquid crystal properties and to understand its correlation with its fire retardant properties.

## 1.4 Objectives

The focus of this research lies in the syntheses of molecules and to observe their mesophase behaviour. This includes:

- a) To synthesise and characterise mono- and bisazobenzene intermediates (series **1-6**) and the final compounds of mono- and hexa-substituted cyclotriphosphazene with monoazobenzene arm (**7a-f**) and bisazobenzene arm (**8a-f**).
- b) To determine the liquid crystalline properties of the intermediates and final products.

## 1.5 Scope of study

The main focus of this project includes the synthesis and characterisation of the intermediates and final compounds of cyclotriphosphazene derivatives with the azo linking unit. Structural confirmation of all the synthesised compounds will be done using Fourier Transform Infrared (FT-IR), 1D and 2D Nuclear Magnetic Resonance (NMR) and CHN Elemental analysis. Determination of their liquid crystal properties will be done using Polarised Optical Microscope (POM) while enthalpy changes of the mesophase transitions will be calculated from the thermogram of Differential Scanning Calorimetry (DSC). All these instruments are located at the School of Chemical Sciences, USM. The correlation between liquid crystallinity with fire retardance properties will be investigated on these cyclotriphosphazene derivatives having the azo linking unit.

## **CHAPTER 2**

### **METHODOLOGY**

#### **2.1 CHEMICALS**

4-aminophenol, sodium nitrite, 37% hydrochloric acid, phenol, potassium hydroxide, sodium hydroxide, potassium carbonate, sodium acetate anhydrous, dichloromethane, bromoheptane, bromodecane, bromododecane, 4-nitroaniline, sodium sulfide nonahydrate, hexachlorocyclotriphosphazene, triethylamine, tetrahydrofuran, ethyl acetate, hexane, acetone, methanol and ethanol were purchased from Merck and Quality Reagent Chemical, QRëC™ and were used without further purification.

#### **2.2 INSTRUMENTS**

##### **2.2.1 Elemental Analysis**

CHN analysis is accomplished by combustion analysis in which a sample is burned in an excess of oxygen, and the masses of the combustion can be used to determine carbon (C), hydrogen (H), and nitrogen (N) in the sample. The percentages of the elements were analysed using CHNS/O Analyser: Perkin Elmer, Series II, 2400.

##### **2.2.2 Infrared (IR) Spectroscopy**

FT-IR is a technique used to identify the functional groups in a sample. The absorption bands correspond to their respective functional groups. Compounds were analysed with Perkin Elmer: FT-NIR Spectrometer Frontier.

### **2.2.3 Nuclear Magnetic Resonance (NMR) Spectroscopy**

NMR spectroscopy is a technique used to determine the molecular structure of a compound for atomic nuclei  $^1\text{H}$  and  $^{13}\text{C}$ . The  $^1\text{H}$  and  $^{13}\text{C}$  NMR spectra were obtained using Bruker 500 MHz Ultrashield<sup>TM</sup>. The sample (20mg) was dissolved in deuterated solvent. The interpretation of the spectra was recorded by chemical shift in ppm (multiplicity = singlet (s), doublet (d), triplet (t), multiplet (m); coupling constant (Hz); integration.

### **2.2.4 Melting point**

Sample was loaded into a melting point capillary which was placed in the apparatus and heated by a heating block. The temperature at which the phase changes from solid to liquid is determined. The melting points were measured using Gallenkamp Melting Point Apparatus.

### **2.2.5 Polarised Optical Microscope (POM)**

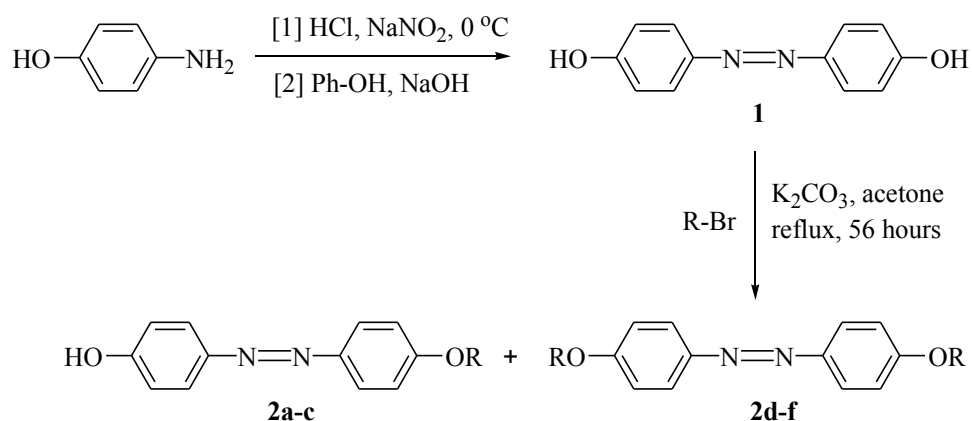
POM is a technique that employs polarised light to detect liquid crystal mesophase(s) whereby sample was placed between two glasses on the hot stage under the microscope. The phase changes of the sample were observed in the heating and cooling cycles, which can be controlled and recorded. The mesophase textures of the compounds were observed using a Carl Zeiss Polarising Optical Microscope equipped to Linkam Scientific Instruments LTS350.

### **2.2.6 Differential Scanning Calorimetry (DSC)**

DSC is a technique in which a sample is heated from a crystal to liquid phase. The energy changes can also be observed during the phase transitions. In the heating and cooling cycles, each phase transition showed a curve on the spectrum, which can be calculated for the enthalpies of transitions. Compounds were tested using Pyris 1, Differential Scanning Calorimetry, Perkin Elmer.

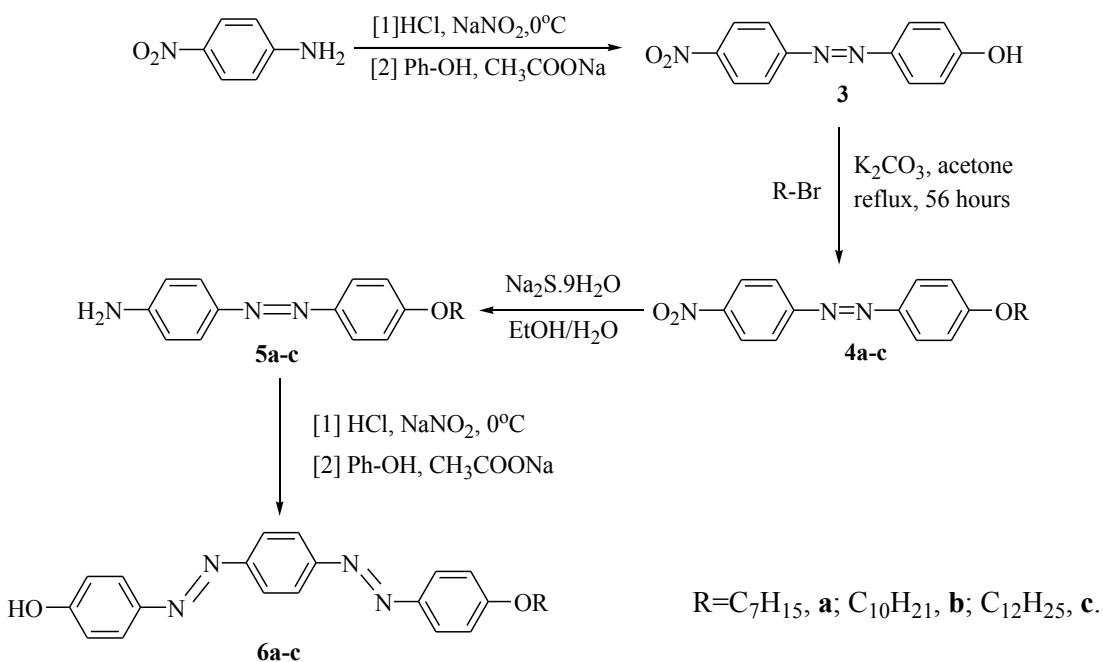
## 2.3 SYNTHESIS METHOD

The synthesis of intermediates and final products are as shown in Schemes 1-6. Thin Layer Chromatography (TLC) was used to monitor the reaction progress and the purity of the products. The eluent used was 15:75 or 20:80 of ethyl acetate:hexane.

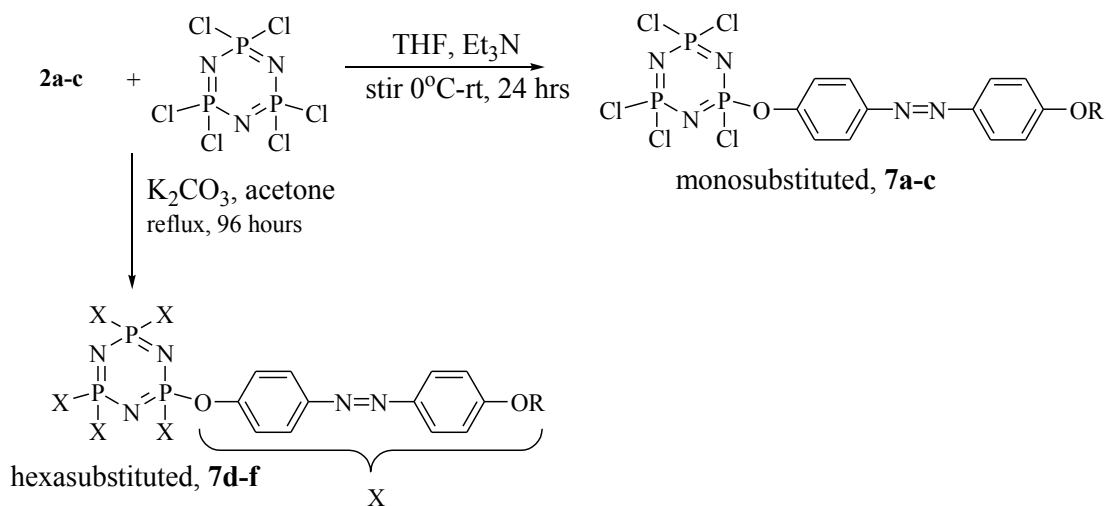


R = C<sub>7</sub>H<sub>15</sub>, **a**; C<sub>10</sub>H<sub>21</sub>, **b**; C<sub>12</sub>H<sub>25</sub>, **c**; C<sub>7</sub>H<sub>15</sub>, **d**; C<sub>10</sub>H<sub>21</sub>, **e**; C<sub>12</sub>H<sub>25</sub>, **f**.

Scheme 1: Synthesis pathway for azo coupling of monoazobenzene, **2a-f**

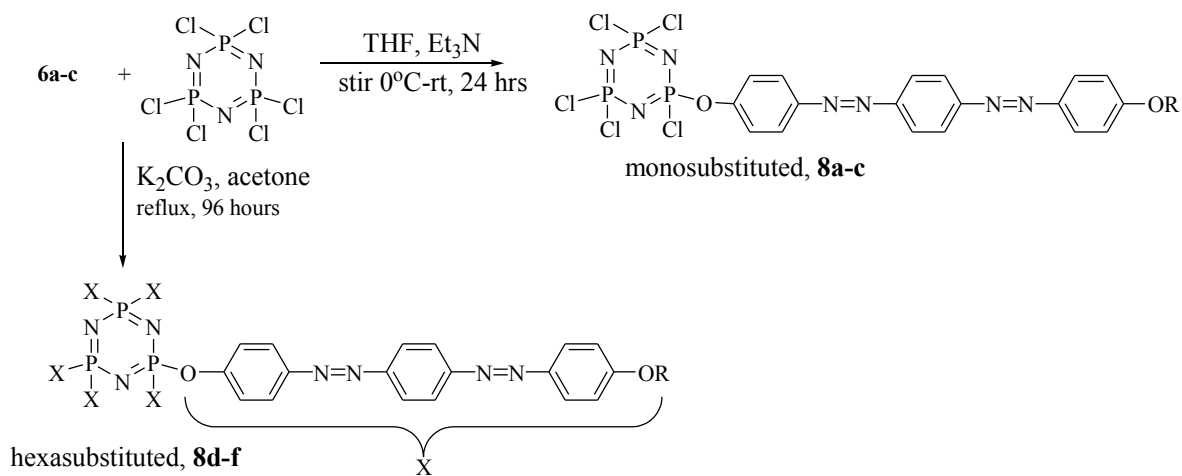


Scheme 2: Synthesis pathway for azo coupling of bisazobenzene, **6a-c**



R = C<sub>7</sub>H<sub>15</sub>, **a**; C<sub>10</sub>H<sub>21</sub>, **b**; C<sub>12</sub>H<sub>25</sub>, **c**; C<sub>7</sub>H<sub>15</sub>, **d**; C<sub>10</sub>H<sub>21</sub>, **e**; C<sub>12</sub>H<sub>25</sub>, **f**.

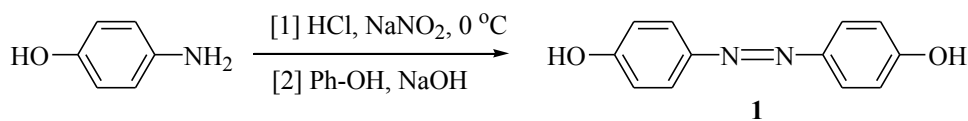
Scheme 3: Synthesis pathway of cyclotriphosphazene products with monoazo linking unit for mono-substituted, **7a-c** and hexa-substituted, **7d-f**



R = C<sub>7</sub>H<sub>15</sub>, **a**; C<sub>10</sub>H<sub>21</sub>, **b**; C<sub>12</sub>H<sub>25</sub>, **c**; C<sub>7</sub>H<sub>15</sub>, **d**; C<sub>10</sub>H<sub>21</sub>, **e**; C<sub>12</sub>H<sub>25</sub>, **f**.

Scheme 4: Synthesis pathway of cyclotriphosphazene products with two azo linking unit for mono-substituted, **8a-c** and hexa-substituted, **8d-f**

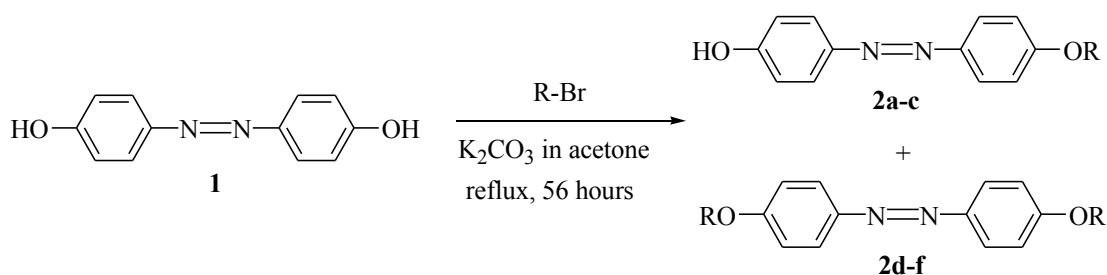
### 2.3.1 Azo coupling of 4,4'-(diazene-1,2-diyl)diphenol, **1**



A solution of 4-aminophenol (0.03 mol) and 50 mL of 1M HCl was cooled to 0°C. NaNO<sub>2</sub> (0.03 mol) in 10 mL of H<sub>2</sub>O was added dropwise into the mixture, followed by 100 mL of methanol (MeOH). A separate mixture of phenol (0.03 mol) and KOH (0.05 mol) was prepared in 20 mL MeOH and was cooled to 0°C. The mixture from the latter was added dropwise into the former and the reaction solution was left to stir for 2 hours at 0°C and another 2 hours at room temperature. Most of the MeOH was removed by evaporation and the residue solution was acidified to pH 4. The resultant precipitate was filtered and washed with distilled water. The precipitate was recrystallised from EtOH/H<sub>2</sub>O mixture and dried under vacuum conditions to give **1** as red precipitate (Alam et.al, 2011).

**Yield:** 96.0%, purplish red solid. **M.p.** 194-196 °C. **<sup>1</sup>H NMR (500 MHz, DMSO-d<sub>6</sub>):** δ, ppm: 10.15 (s, 1H), 7.71 (d, J=9.0 Hz, 2H), 6.91 (d, J=9.0 Hz, 2H). **<sup>13</sup>C NMR (125 MHz, DMSO-d<sub>6</sub>):** δ, ppm: 160.03, 145.32, 124.19, 115.84. **IR (cm<sup>-1</sup>):** 3194 (O-H broad stretch), 2811 (asymmetric C-H stretch), 2709 (symmetric C-H stretch), 1590 (aromatic C=C stretch), 1477, 1429 (N=N stretch), 1250 (C-O stretch), 833 (C-H bend). **CHN elemental analysis:** Calculated for C<sub>12</sub>H<sub>10</sub>O<sub>2</sub>N<sub>2</sub>: C: 67.28%, H: 4.71%, N: 13.08%; Found: C: 66.95%, H: 4.78%, N: 12.98%.

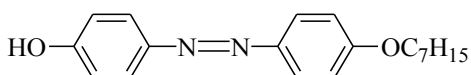
### 2.3.2 General procedure for the alkylation of compounds 2a-f



where R = C<sub>7</sub>H<sub>15</sub>, **a**; C<sub>10</sub>H<sub>21</sub>, **b**; C<sub>12</sub>H<sub>25</sub>, **c**; C<sub>7</sub>H<sub>15</sub>, **d**; C<sub>10</sub>H<sub>21</sub>, **e**; C<sub>12</sub>H<sub>25</sub>, **f**.

A solution of compound **1** (4.12 mmol) and K<sub>2</sub>CO<sub>3</sub> (4.12 mmol) in 50 mL acetone was refluxed for an hour. Bromoalkane (4.76 mmol) was added dropwise to the solution and refluxed for an additional 24 hours. The resultant mixture was suspended in DCM and the inorganic salts were filtered. The filtrate was evaporated and the crude mixture was separated by column chromatography to yield the monosubstituted alkoxy chains **2a-c** and disubstituted alkoxy chains **2d-f** (Kidowaki et. al, 2003).

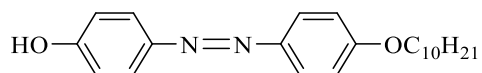
#### 4-(4-Heptyloxyphenylazo) phenol, **2a**



**Yield:** 94.0%, orange solid. **M.p.** 95-96 °C. **<sup>1</sup>H NMR (500 MHz, CDCl<sub>3</sub>):** δ, ppm: 7.85 (d, J=9.0 Hz, 2H), 7.81 (d, J=9.0 Hz, 2H), 6.97 (d, J=9.0 Hz, 2H), 6.90 (d, J=9.0 Hz, 2H), 4.02 (t, J=6.75 Hz, 2H), 1.82-1.78 (m, 2H), 1.49-1.30 (m, 8H), 0.89 (t, J=7.0 Hz, 3H). **<sup>13</sup>C NMR (125 MHz, CDCl<sub>3</sub>):** δ, ppm: 161.66, 158.24, 147.45, 147.06, 124.87, 124.64, 116.08, 115.09, 68.73, 31.99, 29.48, 29.25, 26.22, 22.80, 14.21. **IR (cm<sup>-1</sup>):** 3160-3570 (O-H broad stretch), 2923 (asymmetric C-H stretch), 2858 (symmetric C-H stretch), 1582, 1598 (aromatic C=C stretch), 1471 (N=N stretch), 1239 (C-O stretch), 841 (C-H bend).

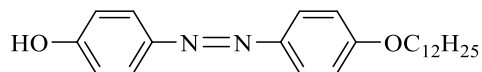


4-(4-Decyloxyphenylazo) phenol, **2b**



**Yield:** 94.9%, orange solid. **M.p.** 105-107 °C. **<sup>1</sup>H NMR (500 MHz, CDCl<sub>3</sub>):** δ, ppm: 7.90 (d, J=9.0 Hz, 2H), 7.88 (d, J=8.0 Hz, 2H), 6.96 (d, J=9.0 Hz, 4H), 4.00 (t, J=6.75 Hz, 2H), 1.82-1.76 (m, 2H), 1.48-1.26 (m, 14H), 0.87 (t, J=7.0 Hz, 3H). **<sup>13</sup>C NMR (125 MHz, CDCl<sub>3</sub>):** δ, ppm: 161.84, 159.42, 146.22, 145.68, 125.53, 124.72, 116.38, 115.08, 68.66, 32.10, 29.77, 29.76, 29.59, 29.53, 29.38, 26.21, 22.89, 14.33. **IR (cm<sup>-1</sup>):** 3164-3571 (O-H broad stretch), 2919 (asymmetric C-H stretch), 2850 (symmetric C-H stretch), 1583, 1598 (aromatic C=C stretch), 1472 (N=N stretch), 1243 (C-O stretch), 841 (C-H bend).

4-(4-Dodecyloxyphenylazo) phenol, **2c**



**Yield:** 90.3%, orange solid. **M.p.** 99-110 °C. **<sup>1</sup>H NMR (500 MHz, CDCl<sub>3</sub>):** δ, ppm: 7.93 (d, J=9.0 Hz, 2H), 7.89 (d, J=7.5 Hz, 2H), 7.01 (d, J=9.0 Hz, 2H), 6.94 (d, J=9.0 Hz, 2H), 4.00 (t, J=7.0 Hz, 2H), 1.82-1.77 (m, 2H), 1.49-1.29 (m, 20H), 0.86 (t, J=7.0 Hz, 3H). **<sup>13</sup>C NMR (125 MHz, CDCl<sub>3</sub>):** δ, ppm: 161.68, 159.38, 146.27, 145.32, 125.56, 124.78, 116.38, 115.07, 68.81, 32.93, 30.68, 30.65, 30.61, 30.56, 30.49, 30.37, 30.21, 27.04, 23.71, 15.34. **IR (cm<sup>-1</sup>):** 3168-3569 (O-H broad stretch), 2918 (asymmetric C-H stretch), 2850 (symmetric C-H stretch), 1583, 1598 (aromatic C=C stretch), 1472 (N=N stretch), 1244 (C-O stretch), 841 (C-H bend). **CHN elemental analysis:** Calculated for C<sub>24</sub>H<sub>34</sub>O<sub>2</sub>N<sub>2</sub>: C: 75.35%, H: 8.96%, N: 7.32%; Found: C: 75.01%, H: 8.62%, N: 7.47%.